



Differential glycosylation expression in injured rat spinal cord treated with immunosuppressive drug Cyclosporin-A.

Title	Differential glycosylation expression in injured rat spinal cord treated with immunosuppressive drug Cyclosporin-A.
Author(s)	Kilcoyne, Michelle;Patil, Vaibhav;O'Grady, Claire;Bradley, Ciara;McMahon, Siobhan S.
Publication Date	2019-02-12
Publisher	American Chemical Society
Repository DOI	10.1021/acsomega.8b02524

Differential glycosylation expression in injured rat spinal cord treated with the immunosuppressive drug Cyclosporin-A

Michelle Kilcoyne¹, Vaibhav Patil², Claire O'Grady³, Ciara Bradley³, Siobhan S. McMahon^{3*}

¹Carbohydrate Signalling Group, Discipline of Microbiology, School of Natural Sciences, National University of Ireland Galway, Galway, Ireland, ²Centre for Research in Medical Devices (CÚRAM), National University of Ireland, Galway, Ireland, ³Discipline of Anatomy and NCBES Galway Neuroscience Centre, College of Medicine Nursing and Health Sciences, National University of Ireland Galway, Galway, Ireland.

***Corresponding author**

Dr Siobhan McMahon, Discipline of Anatomy and NCBES Galway Neuroscience Centre, College of Medicine Nursing and Health Sciences, National University of Ireland Galway, Ireland. EMAIL: siobhan.mcmahon@nuigalway.ie TEL: +353 91492838. FAX: +353 91 494520

Abstract

Glycosylation is ubiquitous throughout the central nervous system and is altered following spinal cord injury (SCI). The glial scar that forms following SCI is composed of several chondroitin sulfate proteoglycans (CSPGs) which are inhibitory to axonal regrowth. Cyclosporin-A (CsA), an immunosuppressive therapeutic, has been proposed as a potential treatment after SCI. We investigated CsA treatment in the spinal cord of healthy, contusion injured and injured CsA-treated rats. Lectin histochemistry using fluorescently labelled lectins, SBA, MAA, SNA-I and WFA, was performed to identify the terminal carbohydrate residues of glycoconjugates within the spinal cord. SBA staining decreased in gray and white matter following spinal cord injury while at the lesion site, staining was increased in CsA-treated animals indicating an increase in galactose and *N*-acetylgalactosamine terminal structures. No significant changes in MAA were observed. WFA staining was abundant in gray matter and observed to increase at the lesion site in agreement with increased expression of chondroitin sulfate proteoglycans. SNA-I stained blood vessels in all spinal cord regions and dual staining identified a subpopulation of astrocytes in the lesion site which expressed α -(2,6)-sialic acid. Glycosylation were altered in injured spinal cord treated with CsA indicating that glycosylation and the alteration of particular carbohydrate structures are important factors to consider in examination of the environment of the spinal cord post injury.

Keywords: Spinal cord injury, glycosylation, Cyclosporin-A, lectins, astrocytes

Introduction

In spinal cord injury (SCI), the primary mechanical trauma is caused by direct physical compression of the spinal cord by fractured and displaced bone fragments. Blood vessels are crushed, causing micro-hemorrhages, neural cell membranes broken and axons are damaged, leading to a loss of functional connections.^{1,2} Secondary injury adds to the complexity of SCI. Neuronal destruction causes the release of toxic chemicals that attack neighboring tissue *via* excitotoxicity and often leads to a wave of apoptosis and free radical-induced lipid oxidation.^{3,4} Inflammation plays an important role in early and late stages of SCI.^{5,6} Cells of the immune system migrate from the periphery through the damaged blood-brain barrier and join the resident glial cells within the spinal cord. A fluid filled cyst forms at the site of injury. Many astrocytes become hypertrophic and adopt a reactive phenotype.⁷ Reactive astrocytes begin to secrete inhibitory extracellular matrix (ECM) molecules, including several chondroitin sulfate proteoglycans (CSPGs), and migrate to the lesion site to build a barrier known as the glial scar.⁸ The glial scar produces a physical and chemical barrier and stops damaged and severed axons from traversing the site of injury to unscarred spinal regions where they could potentially regenerate and reconnect functional spinal circuits.^{9,10} The molecular organization of the scar and the production of inhibitory molecules by astrocytes are contributing factors for regenerative failure after SCI.^{7,8,11}

Glycosylation is ubiquitous throughout the central nervous system (CNS) and plays critical roles in development and normal cellular function. Sialic acids are charged residues which often terminate mammalian cell surface structures, ECM glycoconjugates, and glycolipids. Sialic acids fulfil important functions in the CNS as critical components of gangliosides and the repeating units of polysialic acid.¹² Terminal galactose (Gal) residues interact with galectins (receptors found throughout the cell) on cell surfaces and in the ECM, and exert biological effects. For example, galectin-1 is expressed by reactive astrocytes and

after SCI appears to have a neuroprotective effect mediated by reactive astrocytes.¹³ Various sulfated *N*-acetylgalactosamine (GalNAc) residues comprise one of the two residues of the repeating units of chondroitin sulfate (CS) chains on CSPGs, with the structures and sulfation pattern of the CS repeating units determining function. For example, chondroitin-4,6-sulfate (also known as CS E) is potently inhibitory to axonal growth.¹⁴ Previously, we have shown *in vitro* that neuronal glycosylation in an injured environment returns towards normal with Chondroitinase ABC treatment.¹⁵ Thus, a return to healthy ECM and cellular glycosylation after repair would coincide with resumed normal function in the spinal cord.

Many therapeutic strategies have been proposed in treatment of SCI.¹⁶ Cyclosporin-A (CsA) is an immunosuppressive cyclic peptide that has been shown to have neuroprotective properties by inhibiting calcineurin and the mitochondrial permeability transition pore, reducing lipid peroxidation and releasing neurotrophic factors.¹⁷ Additionally, it is known to induce growth-associated protein-43 (GAP-43) expression which is involved in process extension of neurons.¹⁸ Treatment with CsA leads to improved functional recovery after SCI in rats, and it is frequently combined with neural transplantation to avoid tissue rejection.^{19,20} However, the effect of CsA treatment on tissue and cell glycosylation is unknown.

In this study, we investigated glycosylation *in vitro* using normal (primary) astrocytes and an astrocyte cell line, Neu7, that overexpresses CSPGs. We also examined glycosylation *in vivo* within uninjured rat spinal cord, injured spinal cord and injured spinal cord treated with CsA. In particular, we selected a panel of lectins, carbohydrate binding proteins, to elucidate the presence, localisation and potential alteration of structures containing sialic acid, Gal and GalNAc residues, including CS, in the tissues of the CsA treatment compared to normal and no treatment. To clarify potential interactions and functions of the altered glycosylation expression and their roles in the documented effects of CsA treatment after SCI, we also

explored the relationship between axonal growth, CS expression, astrocytes and sialylation expression using a combination of lectin histochemistry and immunohistochemical strategies.

Results and Discussion

Cells are coated with a layer of carbohydrates of complex structure which facilitates the interaction of the cell with other cells and with their environment. The changes in carbohydrate expression can be examined in different tissues (for example, injured versus uninjured spinal cord tissue) using lectins. Lectin histochemistry for both cells and tissues was also carried out in the presence of haptenic sugars. A reduction in intensity of lectin staining was observed for all lectin staining (not shown) which confirmed carbohydrate-mediated binding of lectins.²¹ This study encompasses a multidisciplinary chemical biology approach to studying tissue regeneration after SCI.

Lectin staining of astrocytes in vitro

To initially screen for differences in carbohydrate expression related to CSPGs and sialylation, protein extracts from two types of astrocytes, primary and Neu7, were made, total cell lysates and extracts enriched for membrane (hydrophobic) and cytosolic (hydrophilic) proteins. Neu7 cells overproduce the inhibitory CSPGs including NG2, the CS-56 antigen and versican and is used to simulate a reactive astrocyte phenotype.²² These protein preparations were fluorescently labelled and incubated on lectin microarrays presenting a panel of five lectins with specificity for terminal Gal and GalNAc residues (SBA and WFA) and sialic acid (MAL-I, MAL-II and SNA-I) (Figure 1).

Comparing astrocyte and Neu7 cell lysates, it is clear that there was an increased expression of Gal and GalNAc terminal residues in Neu7 cell lysates as indicated by increased SBA and WFA binding compared to primary astrocytes (Table 1). This is in agreement with

the overproduction of CSPGs by Neu7. Similarly MAL-I and MAL-II binding to Neu7 cell lysates were increased compared to primary astrocyte lysates, which indicated an increased expression of α -(2,3)-linked sialic acid (Table 1). However, binding to SNA-I was similar for both cell lysates which indicated a similar expression of α -(2,6)-linked sialic acid (Table 1). Relative lectin binding intensities for the cells cytosolic protein-enriched extracts were largely in agreement with the cells lysates, but the lectin binding intensities for the membrane protein-enriched extracts differed (Figure 1). Binding to MAL-I was increased for Neu7 cells compared to primary astrocytes, while binding intensities to MAL-II was similar for the membrane protein-enriched extracts for both cell types, indicating a potentially modest increase of α -(2,3)-linked sialic acid expression in Neu 7 cells compared to primary astrocytes. On the other hand, the binding intensity to SNA-I was greater for the membrane protein-enriched extracts of primary astrocytes compared to Neu7 cells.

The enrichment process used here for cytosolic and membrane protein fractionation is based on relative hydrophobicity and hydrophilicity. Therefore cell surface bound hydrophilic proteins such as CSPGs and mucins can be extracted in to the ‘cytosolic’ fractions, so the protein membrane fractionation in this case can only be taken as an enrichment and may not be truly completely representative of the cell surface protein and proteoglycan population.

Thus, the two cell types were then assessed for more specific surface glycosylation changes by cytohistochemistry on the intact cells using the fluorescein isothiocyanate (FITC)-conjugated lectins SBA, MAA, WFA and SNA-I (Table 1). The *Maackia amurensis* agglutinin (MAA) contains both MAL-I and MAL-II lectins and, as both have binding specificity for terminal α -(2,3)-linked sialic acid, MAA was used in place of MAL-I and –II for histochemistry experiments.²³ Although the differences in secreted CSPGs between primary astrocytes and Neu7 cells have been characterised, to our knowledge the cell surface glycosylation has not been previously profiled. Lectin histochemistry revealed a greater

expression of terminal GalNAc (SBA staining) and/or Gal residues and α -(2,3)-linked sialylation (MAA staining) on Neu7 cells compared to primary astrocytes (Fig. 2A-E). The greater SBA and MAA binding of Neu7 cells compared to primary astrocytes was in agreement with the findings from the lectin microarray profiling of the cell protein extracts. However, there was equivalent expression of α -(2,6)-linked sialic acid on primary astrocytes and Neu7 cells as indicated by SNA-I binding (Fig. 2A, 2F, 2G), which was in agreement with the SNA-I binding of cell lysates on the lectin microarray. WFA binding *in vitro* was the same in primary astrocytes and Neu7 cells (Fig. 2A, 2H, 2I) in contrast to the findings of the protein extracts on the lectin microarray. However, as has been noted above, protein extractions are not completely representative of the molecules actually presented on the cell surface so the cytochemistry observations are more indicative of the cell surface expression. It is notable that the lectins SBA and WFA did not have the same binding pattern to Neu7 cells and primary astrocytes, which indicated that the lectins favoured binding to different carbohydrate structures or presentations. Both SBA and WFA have been previously characterised as having similar binding specificities and affinities for terminal α - and β -linked GalNAc and Gal residues.²⁴ Although it is known that WFA additionally binds to CS and is frequently used as a histochemical marker for PNNs, the exact target structure(s) and sulfation pattern(s) to which this lectin binds in CS is not currently known.^{25,26} Thus it is likely that the additional structures recognised by WFA on the primary astrocytes cell surface are components of CS. Expression of α -(2,6)-linked sialic acid is greater compared to α -(2,3)-linked sialic acid on the primary astrocyte surface.²⁷ Apart from α -(2,8)-linked polysialic acid, α -(2,3)-linked sialic acid is typically predominant in the nervous system and there is very little α -(2,6)-sialylation (Kleene and Schachner, 2004). The presence of α -(2,6)-sialylation on the astrocyte cell surface may be a characteristic of this cell type or characteristic of the cell type under certain conditions, such as in culture.

Lectin staining of spinal cord cryosections

Lectin histochemistry of the spinal cord tissue from the three animal groups, uninjured, injured and injured treated with CsA, were examined. The gray and white matter of the uninjured group had a higher intensity of SBA binding overall compared to the same two regions in the injured and CsA-treated groups (Fig. 3A-E, G and H), which indicated a decreased expression of non-sulfated terminal Gal and/or GalNAc residues in the injured and treated tissues compared to healthy. In addition, the SBA binding intensity of the healthy gray matter was approximately three times the magnitude of the uninjured white matter. At the lesion site, a slight increase in SBA intensity was observed in the gray matter and lesion site of the CsA-treated group compared to the injured group (Fig. 3A, F and I). Lozza *et al.* (2009) showed that SBA stains neuronal cell bodies and not glial cells in young and aged rat spinal cords.²⁸ Although the binding of SBA was significantly higher in Neu7 astrocytes *in vitro* compared to normal primary astrocytes, the same binding profile for this lectin was not observed in the injured spinal cord tissue compared to uninjured. This finding highlights the importance of cautious interpretation when relying on *in vitro* data alone for glycosylation analysis.

MAA lectin staining exhibited no significant change in intensity in the gray and white matter of the injured and CsA-treated group compared to the uninjured group (Fig. 4A-E, G and H), and no overall difference in MAA intensity was observed between the lesions sites of the injured and CsA-treated groups (Fig. 4A, F and I). However, consistent with the greater MAA binding to Neu7 cells compared to primary astrocytes, there was an observed trend of slightly increased MAA binding to the injured and CsA-treated tissue overall compared to uninjured, with the intensity of gray matter and lesion site of CsA-treated tissues approximately twice that of the same areas in injured tissues. There is an increased expression of sialylation, sulfation and fucosylation in tissue and on cell surfaces overall associated with inflammation

which facilitates interactions with selectins, although detailed studies of structural changes over time have not been undertaken in neural tissue.²⁹ Previously, it has been shown that neurite outgrowth from cerebellar neurons was enhanced by the presence of α -(2,3)-sialylation on glial CD24 via lectin-like binding to the L1 adhesion molecule.³⁰

There was also no statistically significant difference in SNA-I staining intensity for the white and gray matter between groups (Fig. 5A-E, G and H). Although an increase in intensity was observed at the lesion site of the CsA-treated group compared to the injured group, which indicated increased expression of α -(2,6)-linked sialic acid, this was also not a significant change (Fig. 5A, F and I). The morphology of cells in SNA-I stained tissue in the gray and white matter of CsA-treated group appeared to resemble glial cells (particularly astrocytes). For this reason dual SNA-I lectin and GFAP immunohistochemical staining was carried out on the injured and CsA-treated group to determine if co-localisation could be observed between SNA-I and astrocytes. In the tissue, SNA-I bound to the endothelial cells of blood vessels in all regions examined as expected³¹ and to only a particular subpopulation of astrocytes in the lesion of the injured (Fig. 6A, B) and CsA-treated groups (Fig. 6C, D) at the lesion site which indicated that a subpopulation of astrocytes expressed α -(2,6)-sialylation. It is well known that GFAP expression increases throughout the lesion border in response to injury.^{32,33} The number of astrocytes have been previously reported to increase at the lesion site of CsA-treated animals compared to untreated injured animals at three weeks post-injury.¹⁸ Previously in a study of rat brain injury, both MAA and SNA-I staining was increased in the injured tissue compared to sham-operated control but neither lectin staining co-localised with astrocyte immunoreactivity. However, polysialic acid did co-localise with both microglia and astrocytes, while SNA-I and MAA both co-localised with Iba-1 immunoreactivity.³⁴ In our study, SNA-I also stained other glial cells aside from astrocytes within the lesion areas, as many stained cells were observed surrounding those co-localised with GFAP. Since GFAP does not stain all of

the cellular processes of astrocytes, this may be the reason for the SNA-I staining surrounding GFAP-positive astrocytes.³⁵ SNA-I also stained neurons in the lesion. The expression of the abnormal α -(2,6)-linked sialic acid motif has been reported on the neuronal cell surface in an *in vitro* injury model environment.¹⁵ Reactive astrocytes are more abundant in the spinal cord lesion at later survival times of 7 to 28 days and mainly surround and enclose tissue with phagocytic macrophages and activated microglia.³⁶ Although we cannot confirm that the astrocyte subpopulation expressing α -(2,6)-linked sialylation are reactive astrocytes, this subpopulation was more frequent at the lesion border in the untreated tissue (Fig. 6A) while this subpopulation was more dispersed in the CsA-treated lesion area (Fig. 6B). In an effort to identify which structure on the astrocyte subpopulation surface may have been modified with α -(2,6)-sialic acid, dual staining for SNA-I and β I-integrin was carried out. There appeared to be some sparse evidence of co-localisation observed (Fig. 7). Different glycosylation of receptors alter the signalling response induced in cells after binding to ligands and may serve to regulate signalling functions *in vivo*. Sialylation and galactosylation of the N-linked oligosaccharides on intercellular adhesion molecule-1 (ICAM-1) enhanced the signalling response in mouse astrocytes.³⁷ The expression of α -(2,6)-sialylation has been previously observed on necrotic and apoptotic cells.³⁸ The β 1 integrin is expressed ubiquitously and can pair with at least twelve different α subunits to bind different ligands and induce a signalling response. Variable glycosylation of β 1 integrin alters binding and signalling response³⁹ and α -(2,6)-sialylation of β 1 integrin has been shown to block binding to Gal-3 and protect colon carcinoma cells against apoptosis.⁴⁰ However, in our study we were unable to co-localise SNA-I and β 1 integrin staining, suggesting that a different receptor or structure was modified on the astrocyte subpopulation expressing α -(2,6)-sialylation in the lesion.

Although similar binding of WFA was observed *in vitro* between normal astrocytes and Neu7 cells in our study, WFA lectin staining was significantly increased in the gray matter

compared to the white matter of the uninjured tissues, at approximately 10 times greater in magnitude. The uninjured gray matter was significantly greater than the gray matter in both the injured and CsA-treated animal groups, while the WFA staining uninjured white matter was significantly less compared to the white matter in the injured and CsA-treated animal group (Fig. 8A-E). A significant increase in WFA binding was also observed at the lesion site compared to gray and white matter in both the injured and the CsA-treated groups, with less binding in the gray matter and lesion site of the CsA-treated group compared to the injured group (Fig. 8A, D-I). Increased expression of CSPGs has been shown within perineuronal nets (PNNs) in CNS lesioned tissue.⁴¹ In a conditional Sox9 knock-out, reduction of CSPGs within PNNs has been shown.⁴² CSPGs are also present in white matter of the spinal cord.⁴³ After SCI, these CSPGs are elevated and cause the inhibition of axonal growth.⁴⁴ Previously, ChABC was injected into the spinal cord near the lesion resulting in degradation of the CSPGs which promoted sprouting of the injured dorsal column axons and functional recovery and also reduced WFA staining of PNNs.⁴⁵ In our study, WFA staining in the lesion site of the CsA-treated tissue was higher in comparison to the gray and white matter. WFA staining at the injury was much lower in the CsA-treated group compared to the injured group with no treatment, indicating CsA may be having an effect on CS expression. As WFA staining is used to stain PNNs, which wrap around neuronal cell bodies or neurons, as well as other CSPGs present.²⁵ Dual WFA lectin and GAP-43 immunohistochemical staining was carried out on the injured (Fig. 8A, B) and CsA-treated group (Fig. 8C, D) at the lesion site to assess the relationship between neurons and WFA. Although both markers stained adjacent and closely related cells, no co-localisation of WFA and GAP-43 was observed. The dual lectin and immunohistochemistry images indicated tissue remodelling in the lesion of the CsA-treated tissue compared to injured tissue (Figs. 7-10), supporting the idea that CsA treatment reduced the formation of the glial scar at the lesion 3 weeks after injury.

As removal of PNNs are associated with a return to plasticity of the neurons and functional recovery, both CsA-treated and injured tissue groups were stained for the presence of neurogranin.⁴⁶ Neurogranin (RC3,BICKS) is a neuron-specific calmodulin-binding protein kinase C substrate found in the neuronal cell body, dendrites and axons and can be associated with neuronal plasticity.⁴⁷ Although dual staining with WFA and anti-neurogranin antibody did not reveal any co-localisation in the injured tissue group (Fig. 10A-C), there did appear to be some co-localisation in the CsA group (Fig. 10D, E), providing further evidence of the beneficial treatment with CsA.

Many studies have been carried out where CsA administration caused functional recovery. The neuroprotective effects of CsA have been well documented (McMahon *et al.*, 2009; Sullivan *et al.*, 2011) and this drug inhibits oxidative free radicals and stabilises the injury environment. The best functional improvement was seen in animals that had CsA administered 6 hours post injury⁴⁸, and CsA treatment has been shown to increase neuronal survival and inhibit demyelination when administered within a day after SCI.^{17,19} When CsA was administered 4 days after injury, after the primary wave of injury had passed, functional improvement was also observed 3 weeks post injury.¹⁸ However, CsA treatment does not always show functional recovery due to calcineurin present in the lesion which inhibits CsA treatment.⁴⁹

In this study, we have shown that glycosylation was altered in injured rat spinal cord with CsA treatment compared to injured tissue with no treatment. While the overall tissue glycosylation did not return to normal conditions, CsA treatment from 4 days to 3 weeks post-injury did appear to significantly lower CSPG expression in the CsA-treated lesion compared to injured tissue and also indicated tissue remodelling. In addition, a subpopulation of astrocytes localised in the lesion expressed α -(2,6)-linked sialylation and these were also present in the CsA-treated lesion tissue. These alterations in glycosylation may contribute to

the functional improvements previously observed for CsA treatment. This study supports the inclusion of glycosylation, a critical component of the CNS, as an important aspect in future research on CNS injury and regeneration to provide a more complete perspective on successful molecular repair and remodelling strategies.

Experimental section

Materials

Culture plastics were from BD Biosciences (San Jose, CA, USA). Fluorescein isothiocyanate (FITC)-conjugated and unlabelled lectins (Table 1) were purchased from EY Labs (San Mateo, CA, USA) except for unlabelled MAL-I and MAL-II, which were from Vector Laboratories Inc. (Burlingame, CA, U.S.A.). Bovine serum albumin (BSA, $\geq 99\%$), rhodamine-conjugated anti-rabbit IgG antibody, mouse monoclonal anti-growth associated protein-43 (GAP-43) antibody and 4',6-diamidino-2-phenylindole (DAPI) were from Sigma-Aldrich Co. (Dublin, Ireland). The BSA was periodate-treated (pBSA) (Glass *et al.*, 1981) and used for all histochemical blocking. The cOmplete™ protease inhibitor cocktail, EDTA-free, (cat. no. 11873580001) and PhosSTOP™ phosphatase inhibitor cocktail were from Roche, Inc. (Basel, Switzerland). The Pierce™ bicinchoninic acid (BCA) assay kit and Mem-PER™ Plus membrane protein extraction kit were from Thermo Fisher Scientific™ (Waltham, MA, U.S.A.) The carboxylic acid succinimidyl ester Alexa Fluor® 555 (AF555) fluorescent label, ProLong® Gold antifade and Alexa Fluor® 594 conjugated goat anti-mouse IgG antibody were from Life Technologies (Grand Island, NY, USA). Amicon Ultracel 3 kDa molecular weight cut off (MWCO) centrifugal ultrafiltration units were supplied by Millipore (Cork, Ireland). The rabbit polyclonal anti-glial fibrillary acidic protein (GFAP) antibody was from DakoCytomation (Dublin, Ireland), the rabbit polyclonal anti-neurogranin antibody from

Abcam (Cambridge, U.K.), and the mouse monoclonal anti- β I-integrin antibody were from Chemicon International Inc. (Temecula, CA, USA). Nexterion® Slide H microarray slides were supplied by Schott AG (Mainz, Germany). The 8-well gasket slide and incubation cassette system was from Agilent Technologies Ireland, Ltd., (Cork, Ireland). All other reagents were from Sigma Aldrich Co. (Dublin, Ireland) unless otherwise indicated, and were of the highest grade available.

Cell culture

Primary cerebral astrocytes for immunocytochemistry were obtained from P2 Sprague Dawley rat pups, and were purified and cultured as previously described.^{15,50} For protein extracts, primary astrocytes were prepared from spinal cords isolated from 3-4-day old postnatal Sprague Dawley rats. Spinal cords were isolated by minor modification of the 'Ejection method'.⁵¹ Briefly, after decapitation, a transverse cut was made at the lower lumbar region of the spine and spinal cords were flushed through the spinal canal using 19-gauge needle attached to a syringe filled with Hanks' Balanced Salt Solution. Spinal cords were transferred immediately into containing Dulbecco's Modified Eagle's Medium (DMEM)-high glucose supplemented with 1% penicillin and streptomycin (P/S) on ice. Spinal cords were transferred to a petri dish containing the same media and meninges were gently peeled under microdissection microscope. Spinal tissues were chopped into fine (approximately 1 mm) pieces and digested using 1% trypsin-EDTA solution at 37°C for 15-20 min. Trypsin activity was inhibited using DMEM-high glucose supplemented with 10% fetal bovine serum and 1% P/S, and digested tissue was triturated by passing it through various sizes of needles (18-23 gauge). Digested tissue was expelled through a cell strainer filter (70 μ m mesh size, Falcon™) to eliminate clumped cells or undigested tissue.

Neu7 astrocytes (generously provided from Professor James Fawcett⁵²) were cultured in DMEM supplemented with 10% horse serum, 1% L-glutamine and 1% P/S at 37 °C in a 5% humidified CO₂ atmosphere. Primary astrocytes and Neu7 astrocytes were seeded at a density of 10,000 cells onto sterile coverslips in a 12 well tray and grown for 4 days *in vitro*.

Spinal cord injury

Female Sprague Dawley rats (Charles River UK Ltd, Margate, UK) weighing between 220-225 grams were used in this study. Rats were housed with a 12 hour light/dark cycle in a temperature-controlled room. Food and water were provided *ad libitum*. All animal experiments were carried out in accordance with the Council Directive 2010/63EU of the European Parliament. All housing and surgical procedures carried out in this study were approved by the Animal Care Research Ethics Committee at the National University of Ireland, Galway and the Health and the Health Products Regulatory Authority. Nine female Sprague Dawley rats were used in this study. Three animals were used as control (uninjured) rats and six rats received a SCI. Prior to surgery rats were weighted and pre-operative analgesia, Buprenorphine (0.1-0.025 mg/kg, FortDodge Animal Health Ltd) was delivered intraperitoneal (IP). The rats were anaesthetised by IP injection of Ketamine and Xylazine (100 and 10 mg/kg, respectively) following which a laminectomy was performed at T8-T10. Injured animals received a 200 kilodyne moderate contusion injury at T9 using an Infinite Horizon Impactor Device (Precision Systems and Instrumentation, Lexington, KY, USA). The muscle and skin was sutured with absorbable suture material (Vicryl, 4 metric) and animals kept warm on a heated blanket until fully recovered from intervention. Each animal received a subcutaneous injection of 5-10mg/kg Enrofloxacin (Baytril[®] 5%, Bayer) antibiotic once daily for a minimum period of a week. Pain relief was provided by administering buprenorphine (Torbugesic[®], FortDodge Animal Health Ltd.) at 0.1-0.25 mg/kg twice daily for 7 days after surgery. Saline

solution (3.5ml) was administered subcutaneously for 3 days following surgery. Bladders were manually expressed twice daily from day of injury.

CsA administration

The six injured animals were randomly divided into two groups: a CsA-treated group (n= 3) and a control group (n= 3). A subcutaneous injection of 5 mg/kg CsA (Sandimmun[®], Sandoz) was administered 4 days post-injury to the CsA-treated group and every day thereafter for the duration of the experiment.

Tissue processing

Three weeks from the time of injury, all animals were deeply anaesthetised by I.P. injection of Sodium Pentobarbital (50 mg/kg) and perfused transcardially with saline followed by 4% paraformaldehyde in 0.01 M phosphate buffered saline, pH 7.4 (PBS). Spinal cords were dissected out, post-fixed overnight with 4% paraformaldehyde, immersed in 30% sucrose overnight and frozen in liquid nitrogen-chilled Isopentane. Spinal cords were cryosectioned transversely at 20 µm thickness in a rostral to caudal direction.

Cell protein extractions and fluorescent labelling

Primary astrocytes and Neu7 cells (5×10^6 cells/mL) were lysed to make total protein lysate in a radioimmunoprecipitation assay (RIPA) buffer (50 mM Tris-HCl, 150 mM NaCl, 0.02% sodium azide, 0.1% sodium dodecyl sulphate, 1% Nonidet P-40, 0.5% sodium deoxycholate, pH 8.0,) with cOmplete[™] protease inhibitor cocktail, EDTA-free, (1:100), phenylmethylsulfonylfluoride (1:50) and PhosSTOP[™] phosphatase inhibitor cocktail (1:10). Cells were also fractionated using the Mem-PER[™] Plus membrane protein extraction kit (Thermo Fisher Scientific) in to membrane (hydrophobic) and cytosolic (hydrophilic) protein-

enriched fractions according to manufacturer's instructions. The protein concentrations of the total cell lysate, cytosolic protein fraction and membrane protein fraction was determined using a Pierce™ BCA assay kit and a BSA standard. Protein preparations were then aliquoted and stored at -80°C until further use.

Protein extracts (200 µg) were labelled with AF555 (λ_{ex} 555 nm, λ_{em} 580 nm) in 250 mM sodium borate, pH 8.3, in the dark essentially as previously described.⁵³ Briefly, 1 mg of AF555 was dissolved in 100 µL dimethylsulfoxide and 5 µL of the dissolved dye was added to each sample in a final volume of approximately 300 µL and incubated at 25 °C for 2 h in the dark at room temperature. Labelled protein samples were then purified and buffer exchanged in PBS using a 3 kDa MWCO centrifugal filters. Labelled protein samples were quantified for protein content and substitution according to manufacturer's instructions and samples were stored in the dark at 4 °C until further use.

Lectin microarray construction, incubation and data extraction

A panel of 5 unlabelled pure lectins, MAL-I, MAL-II, SBA, WFA and SNA-I, were prepared at 0.5 mg/mL in PBS, pH 7.4, supplemented with 1 mM of the appropriate haptenic sugar (Table 1). Lectins were printed at approximately 1 nL per feature on Nexterion® Slide H microarray slides using a sciFLEXARRAYER S3 piezoelectric printer (Scienion AG, Berlin, Germany) as previously described.⁵³ Each microarray slide contained eight replicate subarrays, with each lectin spotted in replicates of six per subarray. To ensure complete conjugation, these slides were then incubated in a humidity chamber overnight at room temperature. Residual functional groups were deactivated by incubation in 100 mM ethanolamine in 50 mM sodium borate, pH 8.0, for 1 h at room temperature. Each slide was washed with PBS, pH 7.4, containing 0.05% Tween® 20 three times for 3 min per wash, once with PBS, centrifuged dry (450 x g, 5 min) and stored at 4 °C with desiccant until use.

Prior to use, the lectin microarray slides were allowed to equilibrate to room temperature for 30 min with desiccant. Microarrays were protected from light throughout the procedure. Fluorescently-labelled protein samples were diluted in Tris-buffered saline supplemented with Ca^{2+} and Mg^{2+} ions (TBS; 20 mM Tris-HCl, 100 mM NaCl, 1 mM CaCl_2 , 1 mM MgCl_2), pH 7.2, with 0.05% Tween®-20 (TBS-T) for incubation on the microarray slides. Initially, two fluorescently-labelled protein samples were titrated (1 – 10 $\mu\text{g}/\text{mL}$) to determine the optimal concentration for signal to background ratio. For triplicate experiments, the optimal concentration of 2 $\mu\text{g}/\text{mL}$ of each labelled sample in TBS-T was incubated on three separate microarray slides. For incubations, 70 μL of each diluted sample was applied to each well of the gasket slide, sandwiched with the lectin microarray in an incubation cassette system (Agilent Technologies) and incubated in the dark (1 h, 23 °C, 4 rpm) essentially as previously described.⁵³ Following incubation, microarrays were washed twice in TBS-T and once in TBS for 3 min each wash. Finally, microarrays were dried by centrifugation and imaged in an Agilent G2505B (Agilent Technologies) microarray scanner using the green channel (532 nm excitation, 90% PMT, 5 μm resolution). Images were stored as high resolution .tif files.

Microarray data extraction from image files was performed essentially as previously described⁵³ using GenePix Pro v6.1.0.4 (Molecular Devices, Berkshire, U.K.). The data was then exported as text to Excel (version 2010, Microsoft). Local background-corrected median feature intensity data (F532median-B532) values were selected and the median of six replicate spots per subarray was handled as a single data point for graphical analysis. Binding intensity data is represented in bar charts as the mean intensity with single standard deviation of all like experimental replicates.

Lectin cytochemistry

Lectin cytochemistry was performed at room temperature on primary astrocytes and Neu7 astrocytes. Cells were fixed with 4% paraformaldehyde in PBS for 10 minutes and washed four times in Tris-buffered saline (TBS) supplemented with 1 mM each of the divalent cations Ca^{2+} and Mg^{2+} necessary for lectin function for 2 minutes each wash. pBSA was used for all histochemical blocking.⁵⁴ The cells were blocked with 2% pBSA in TBS for 30 min, washed four times in TBS and then incubated with 20 $\mu\text{g}/\text{mL}$ in TBS of the FITC-conjugated SNA-I, MAA, WFA or SBA lectins (Table 1) for 1 hour in the dark. Inhibitory controls were also carried out in parallel to ensure that lectin binding was carbohydrate-mediated (Gerlach, *et al.*, 2011). Inhibition was done by pre-incubating lectins with 100 mM of the appropriate haptenic carbohydrates in TBS for 1 hour prior to cell staining (SNA-I and MAA in lactose and WFA and SBA in GalNAc) and lectin incubation was also carried out in the presence of the appropriate haptenic sugar. After lectin incubation, the cells were washed twice in TBS and incubated with DAPI for 5 minutes (1 $\mu\text{g}/\text{ml}$ in TBS). The cells were washed four times in TBS and mounted on glass slides with a drop of ProLong® Gold antifade reagent (Life Technologies, Grand Island, NY, USA). Images were captured on a Nikon Eclipse E400 fluorescent microscope at 40X magnification and stored digitally for further image analysis.

Lectin histochemistry of tissues

Lectin histochemistry was carried out on three slides from all animals within the three experimental groups. The frozen sections were rehydrated in TBS containing 0.05% Triton X-100 (TBS-T2) and washed twice in TBS-T for 2 minutes each wash. The sections were blocked with 2% pBSA in TBS-T2 for 1 hour at room temperature and then washed twice. From this point all, all staining procedures were carried out in the dark at room temperature. The sections were then incubated with 20 $\mu\text{g}/\text{ml}$ of FITC-conjugated SNA-I, MAA, WFA or SBA in TBS-T2 for 2 h. The sections were washed three times in TBS-T2 for 2 min each, followed by a

final wash in TBS, and the slides were then cover slipped with ProLong® Gold antifade reagent. Inhibitory controls were carried out in parallel as described above. Images were captured on a Nikon Eclipse E400 fluorescent microscope at 40X magnification and stored digitally for subsequent image analysis.

Dual lectin and immuno-histochemistry of tissues

For lectin and immuno-histochemistry double staining, immediately after the final TBS wash step in the lectin histochemistry method (as above) and continuing the staining procedures in the dark at room temperature, the spinal cord sections were rehydrated in 0.01 M PBS and then blocked with 20% NGS (Sigma-Aldrich Co., Dublin, Ireland). in PBS containing 0.2% Triton X-100 for 20 minutes. The primary antibodies rabbit polyclonal anti-GFAP, 1:300 dilution; DakoCytomation, Dublin, Ireland), rabbit polyclonal anti-neurogranin (1:100), mouse monoclonal anti- β I-integrin (1:100), rabbit polyclonal anti-growth associated protein 43 (GAP-43, 1:100) was diluted in PBS containing 2% NGS and 0.02% Triton X-100 and sections were incubated with the primary antibody for 2 hours. Sections were washed three times in PBS and the appropriate secondary antibody, anti-rabbit IgG conjugated to rhodamine or anti-mouse conjugated to Alexa Fluor® 594 (Life Technologies, Grand Island, NY, USA) was diluted 1:500 in PBS and incubated for 1 hour. Sections were again washed in PBS and cover slipped with ProLong® Gold antifade reagent. A negative control was carried out for each antibody by substituting PBS for the primary antibody. Images were captured on an Olympus IX81 fluorescent microscope at 20X and 40X magnification and stored digitally for further image analysis.

Image analysis

Three images were captured at the same exposure time from each coverslip containing primary astrocytes and Neu7 astrocytes for each lectin stain. The images were then analysed for the integrated density of green fluorescence (lectin binding) using Image Pro[®] Plus software (Media Cybernetics, Silver Springs, MD). The quantity of green fluorescence was compared to the number of cells present using the DAPI images to count cell numbers and give the integrated density reading per cell.

Three images were captured from both the white matter and gray matter of the uninjured animal group and from the white matter, gray matter and lesion site of the injured animal groups for all three lectins. Images were captured at the same exposure time for each region of interest and animal group examined. For each region of interest, the images were randomly chosen. Image Pro[®] Plus was again used to acquire the integrated density of lectin binding from the digital images. For some of the images, the brightness and contrast have been enhanced using Adobe Photoshop CS2 9.0 to allow for easier identification of positively stained tissue.

Statistical analysis

The average integrated density of lectin staining *in vitro* and *in vivo* for each sampling region was calculated using Microsoft Excel v. 2007 and standard error of the mean (SEM) was calculated. Statistical calculations were performed using Minitab 16 software (Minitab Ltd., Coventry, U.K.). A two way analysis of variance (ANOVA) was performed to examine differences between regions of interest and treatment groups. *Post hoc* comparisons were undertaken by Fisher's test. Differences were considered to be statistically significant at a probability value (P) ≤ 0.05 .

List of abbreviations

ANOVA, analysis of variance; BLBP, brain lipid binding protein; BSA, bovine serum albumin; CNS, central nervous system; CsA, Cyclosporin-A; DAPI, diamidino-2-phenylindole; DMEM, Dulbecco's Modified Eagle's Medium; ECM, extracellular matrix; FITC, fluorescein isothiocyanate; GAP-43, growth-associated protein-43; GFAP, glial fibrillary acidic protein; IP, intraperitoneal; *P*, probability value; pBSA, periodate-treated; PBS, phosphate buffered saline; PNNs, perineuronal nets; P/S, penicillin and streptomycin; RIPA, radioimmunoprecipitation assay; SCI, spinal cord injury; SEM, standard error of the mean; TBS, Tris-buffered saline; TBS-T, TBS with 0.05% Tween-20; TBS-T2, TBS with 0.05% Triton X-100.

Acknowledgment

This work was supported by the EU FP7 programme in support of GlycoHIT (grant number 260600) and Science Foundation Ireland (grant number 13/RC/2073) in support of the Centre for Research in Medical Devices (CÚRAM). MK is grateful to the Royal Society of Chemistry Analytical Chemistry Trust Fund (ACTF) for the ACTF Fellowship 2018. The authors acknowledge the facilities, scientific and technical assistance (Mr Mark Canney and Dr Kerry Thompson) of the Centre for Microscopy and Imaging at the National University of Ireland Galway (www.imaging.nuigalway.ie), a facility which is co-funded by the Irish Government's Programme for Research in Third Level Institutions, Cycles 4 and 5, National Development Plan 2007-2013.

Author information

Michelle Kilcoyne, Carbohydrate Signalling Group, Discipline of Microbiology, School of Natural Sciences, National University of Ireland Galway, University Road, Galway, Ireland, H91 TK33. Email: michelle.kilcoyne@nuigalway.ie

Claire O’Grady, Discipline of Anatomy and NCBES Galway Neuroscience Centre, College of Medicine Nursing and Health Sciences, National University of Ireland Galway, University Road, Galway, Ireland, H91 TK33. Email: claireogrady1@gmail.com

Ciara Bradley, Discipline of Anatomy and NCBES Galway Neuroscience Centre, College of Medicine Nursing and Health Sciences, National University of Ireland Galway, University Road, Galway, Ireland, H91 TK33. Email: Ciara.cayden@gmail.com

Siobhan S. McMahon, Discipline of Anatomy and NCBES Galway Neuroscience Centre, College of Medicine Nursing and Health Sciences, National University of Ireland Galway, University Road, Galway, Ireland, H91 TK33. Email: Siobhan.mcmahon@nuigalway.ie

Conflict of interest disclosure

The authors declare no competing financial interest.

Data availability

Data will be made available upon request.

References

1. Belegu V, Oudega M, Gary DS, McDonald JW. 2007. Restoring function after spinal cord injury: promoting spontaneous regeneration with stem cells and activity-based therapies. *Neurosurg Clin N Am* 18:143-68.
2. McDonald JW, Sadowsky C, 2002. Spinal Cord Injury. *The Lancet* 359:417-425.

3. Beattie MS, Farooqui AA, Bresnahan JC. 2000. Review of current evidence for apoptosis after spinal cord injury. *J Neurotrauma* 17:915–26.
4. Liu XZ, Xu XM, Hu R, Du C, Zhang SX, McDonald JW, Dong HX, Wu YJ, Fan GS, Jacquin MF, Hsu CY, Choi DW. 1997. Neuronal and glial apoptosis after traumatic spinal cord injury. *J Neurosci* 17:5395–5406.
5. Benowitz LI, Popovich PG. 2011. Inflammation and axon regeneration. *Curr Opin Neurol* 24:577-83.
6. Fleming JC, Norenberg MD, Ramsay DA, Dekaban GA, Marcillo AE, Saenz AD, Pasquale-Styles M, Dietrich WD, Weaver L.C. 2006. The cellular inflammatory response in human spinal cords after injury. *Brain* 129:3249–3269.
7. Fitch MT, Silver J. 2008. CNS injury, glial scars, and inflammation: Inhibitory extracellular matrices and regeneration failure. *Exp Neurology* 209:294–301
8. Silver J, Miller JH. 2004. Regeneration beyond the glial scar. *Nature Rev Neurosci* 5:146–156.
9. Fitch MT, Silver J. 1997. Glial cell extracellular matrix: boundaries for axon growth in development and regeneration. *Cell Tissue Res* 290:379-384.
10. Oudega, M., 2007. Schwann cell and olfactory ensheathing cell implantation for repair of the contused spinal cord. *Acta Physiol* 189:181–189.
11. Fawcett JW. 2006. Overcoming inhibition in the damaged spinal cord. *J Neurotrauma* 23:371–383.
12. Schnaar, R.L., Gerardy-Schahn, R., Hildebrandt, H. 2014. Sialic acids in the brain: gangliosides and polysialic acid in nervous system development, stability, disease, and regeneration. *Physiol Rev* 94:461-518.

13. Han H, Xia Y, Wang S, Zhao B, Xun Z, Yuan L. 2011. Synergistic effects of galectin-1 and reactive astrocytes on functional recovery after contusive spinal cord injury. *Arch Orthop Trauma Surg* 131:819-839.
14. Brown JM, Xia J, Zhuang BQ, Cho KS, Rogers CJ, Gama CI, Rawat M, Tully SE, Uetani N, Mason DE, Tremblay ML, Peters EC, Habuchi S, Chen DF, Hsieh-Wilson, L. A sulfated carbohydrate epitope inhibits axon regeneration after injury. 2012. *Proc Nat Acad Sci (USA)* 109:4768-4773.
15. Kilcoyne M, Sharma S, McDevitt N, O'Leary C, Joshi L, McMahon SS. 2012 Neuronal glycosylation differentials in normal, injured and chondroitinase-treated environments. *Biochem Biophys Res Commun* 420:616-622.
16. Tohda C, Kuboyama T. 2011. Current and future therapeutic strategies for functional repair of spinal cord injury. *Pharmacol Ther* 132:57-71.
17. Sullivan PG, Sebastian AH, Hall ED. 2011. Therapeutic window analysis of the neuroprotective effects of Cyclosporine A after traumatic brain injury. *J Neurotrauma* 28:311-318.
18. McMahon SS, Albermann S, Rooney GE, Moran C, Hynes J, Garcia Y, Dockery P, O'Brien T, Windebank AJ, Barry FP. 2009. Effect of cyclosporin A on functional recovery in the spinal cord following contusion injury. *J Anat* 215:267-279.
19. Lü H-Z, Wang Y-X, Zhou J-S, Wang F-C, Hu J-G. 2010. Cyclosporin A increases recovery after spinal cord injury but does not improve myelination by oligodendrocyte progenitor cell transplantation. *BMC Neurosci* 11:127-143.
20. McMahon, S.S., Albermann, S., Rooney, G.E., Shaw, G., Garcia, Y., Sweeney, E., Hynes, J., Dockery, P., O'Brien, T., Windebank, A.J., Allsop, T.E., Barry, F.P. 2010. Engraftment, migration and differentiation of neural stem cells in the rat spinal cord following contusion injury. *Cytherapy*, 12:313-325.

21. Gerlach JQ, Kilcoyne M, Eaton S, Bhavanandan V, Joshi L. 2011. Non-carbohydrate-mediated interaction of lectins with plant proteins. *Adv Exp Med Biol* 705:257-269.
22. Fidler PS, Schuette K, Asher RA, Bobbertin A, Thorton SR, Calle-Patino Y, Muir E, Levine JM, Geller HM, Rogers JH, Faissner A, Fawcett JW. 1999. Comparing astrocytic cell lines that are inhibitory or permissive for axon growth: the major axon-inhibitory proteoglycan is NG2. *J Neurosci* 19:8778-8788.
23. Geisler C, Jarvis DL. 2011. Effective glycoanalysis with *Maackia amurensis* lectins requires a clear understanding of their binding specificities. *Glycobiology* 21: 988-993.
24. Piller V, Piller F, Cartron JP. 1990. Comparison of the carbohydrate-binding specificities of seven *N*-acetyl-D-galactosamine-recognising lectins. *Eur J Biochem* 191:461-166.
25. Slaker ML, Harkness JL, Sorg BA. 2016. A standardized and automated method of perineuronal net analysis using *Wisteria floribunda* agglutinin staining intensity. *IBRO Reports* 1:54-60.
26. Irvine SF, Kwok JCF. 2018. Perineuronal Nets in Spinal Motoneurons: Chondroitin Sulphate Proteoglycan around Alpha Motoneurons. *Int J Mol Sci* 19(4): 1172.
27. Kleene R, Schachner M. 2004. Glycans and neural cell interactions. *Nat Rev Neurosci* 5:195-208.
28. Lozza FA, Chinchilla LA, Barbeito CG, Goya RG, Gimeno EJ, Portiansky EL. 2009. Changes in carbohydrate expression in the cervical spinal cord of rats during aging. *Neuropathology* 29(3):258-262.
29. Dube DH, Bertozzi CR. 2005. Glycans in cancer and inflammation – Potential for therapeutics and diagnostics. *Nat Rev Drug Discov* 4:477-488.
30. Lierberoth A, Splittstoesser F, Katagihallimath N, Jakovcevski I, Loers G, Ranscht B, Karagogeos D, Schachner M, Kleene R. 2009. Lewis x and α 2,3-sialyl glycans and

- their receptors TAG-1, contactin, and L1 mediate CD24-dependent neurite outgrowth. *J Neurosci* 29:6677-6690.
31. Lawrenson JG, Cassella JP, Hayes AJ, Firth JA, Allt G. 2000. Endothelial glycoconjugates: a comparative lectin study of the brain, retina and myocardium. *J Anat* 196:55-60.
 32. Renault-Mihara F, Okada S, Shibata S, Nakamura M, Toyama Y, Okano H. 2008. Spinal cord injury: emerging beneficial role of reactive astrocytes' migration. *Int J Biochem Cell Biol* 40:1649-1653.
 33. White RE, McTigue DM, Jakeman LB. 2010. Regional heterogeneity in astrocyte responses following contusive spinal cord injury in mice. *J Comp Neurol* 518(8):1370-1390.
 34. Pacini A, Duchini PP, Bonaccini L, Di Cesare Mannelli L, Selmi V, Adembri C, Vitali L, Sgambati E. 2012. Sepsis worsens the neurological outcome of traumatic brain injury: role of sialic acids related to glial activation. *Italian J Anat Embryol*
 35. Sun D, Jakobs TC. 2012. Structural remodeling of astrocytes in the injured CNS. *Neuroscientist*. 18:567-588.
 36. Popovich PG, Wei P, Stokes BT. 1997. Cellular inflammatory response after spinal cord injury in Sprague-Dawley and Lewis rats. *J Comp Neurol* 377:443-464.
 37. Otto VI, Schürpf, T, Folkers G, Cummings RD. 2004. Sialylated complex-type N-glycans enhance the signalling activity of soluble intercellular adhesion molecule-1 in mouse astrocytes. *J Biol Chem* 279:35201-35209.
 38. Malagolini N, Chiricolo M, Marini M, Dall'Ollio F. 2009. Exposure of α 2,6-sialylated lactosaminic chains marks apoptotic and necrotic deaths in different cell types. *Glycobiol* 19:172-181.
 39. Bellis SL. 2004. Variant glycosylation: an underappreciated regulatory mechanism for α 1 integrins. *1663:52-60*.

40. Zhuo Y, Chammas R, Bellis SL. 2008. Sialylation of $\alpha 1$ integrins blocks cell adhesion to galectin-3 and protects cells against galectin-3-induced apoptosis. *J Biol Chem* 283:22177-22185.
41. Massey JM, Hubscher CH, Wagoner MR, Decker JA, Amps J, Silver J, Onifer SM. 2006. Chondroitinase ABC digestion of the perineuronal net promotes functional collateral sprouting in the cuneate nucleus after cervical spinal cord injury. *J Neurosci* 26(16):4406-4414.
42. McKillop WM, Dragan M, Schedl A, Brown A. 2013. Conditional Sox9 ablation reduces chondroitin sulfate proteoglycan levels and improves motor function following spinal cord injury. *Glia* 61(2):164-177.
43. Tang X, Davies JE, Davies SJ. 2003. Changes in distribution, cell associations, and protein expression levels of NG2, neurocan, phosphacan, brevican, versican V2, and tenascin-C during acute to chronic maturation of spinal cord scar tissue. *J Neurosci Res*. 71(3):427-444.
44. Baldwin KT, Giger RJ. 2015. Insights into the physiological role of CNS regeneration inhibitors. *Front Mol Neurosci*. 8:23.
45. Karetko M, Skangiel-Kramska J. 2009. Diverse functions of perineuronal nets. *Acta Neurobiol Exp (Wars)* 69(4):564-577.
46. van't Spijker, HM, Kwok JCF. 2017. A sweet talk: The molecular systems of perineuronal nets in controlling neuronal communication. *Front Integr Neurosci* 11:33.
47. Houben MPWA, Lankhorst AJ, van Dalen JJW, Veldman H, Joosten EAJ, Hamer FPT, Gispen WH, Schrama LH. 2000. Pre- and post-synaptic localisation of RC3/neurogranin in the adult rat spinal cord: An immunohistochemical study. *J Neurosci Res* 59:750-759.

48. Diaz-Ruiz A, Vergara P, Perez-Severiano F, Segovia J, Guizar-Sahagún G, Ibarra A, Ríos C. 2005. Cyclosporin-A inhibits constitutive nitric oxide synthase activity and neuronal and endothelial nitric oxide synthase expressions after spinal cord injury in rats. *Neurochem Res* 30(2):245-251.
49. Olson EN, Williams RS. 2000. Calcineurin signaling and muscle remodeling. *Cell* 101(7):689-692
50. Donnelly EM, Strappe PM, McGinley LM, Madigan NN, Geurts E, Rooney GE, Windebank AJ, Fraher J, Dockery P, O'Brien T, McMahon SS. 2010. Lentiviral vector-mediated knockdown of the neuroglycan 2 proteoglycan or expression of neurotrophin-3 promotes neurite outgrowth in a cell culture model of the glial scar. *J Gene Med* 12:863-872.
51. Kennedy HS, Jones C, Caplazi P. 2013. Comparison of standard laminectomy with an optimized ejection method for the removal of spinal cords from rats and mice. *J Histotechnol* 36:86-91.
52. Fok-Seang J, Smith-Thomas LC, Meiners S, Muir E, Du JS, Housden E, Johnson AR, Faissner A, Geller HM, Keynes RJ, Rogers JH, Fawcett JW. 1995. An analysis of astrocytic cell lines with different abilities to promote axon growth, *Brain Res* 689: 207–223.
53. Gerlach JQ, Kilcoyne M, Joshi L. 2014. Microarray evaluation of the effects of lectin and glycoprotein orientation and data filtering on glycoform discrimination. *Anal Methods* 6:440-449.
54. Glass WF, Briggs RC, Hnilica LS. 1981. Use of lectins for detection of electrophoretically separated glycoproteins transferred onto nitrocellulose sheets. *Anal Biochem* 115:219-224.

Figure captions

Figure 1

Intensity of primary astrocyte and Neu7 cell protein extracts binding to lectins on microarray.

Bar chart representing the differences in binding of fluorescently labelled protein extracts to printed lectins on a microarray surface where Ast_Lys is total lysate from primary astrocytes, Ast_Cyt is cytosolic (hydrophilic) protein-enriched extract from primary astrocytes, Ast_Mem is membrane (hydrophobic) protein-enriched extract from primary astrocytes, Neu7_Lys is total lysate from Neu7 cells, Neu7_Cyt is cytosolic (hydrophilic) protein-enriched extract from Neu7 cells, and Neu7_Mem is membrane (hydrophobic) protein-enriched extract from Neu7 cells. Bars represent the mean of three replicate experiments (except for duplicate experiments for Neu7_Mem binding to MAL-II), with each experiment the median of six individual replicates. Error bars represent +/- one standard deviation of the mean of the three experiments.

Figure 2

Intensity of lectin staining in primary astrocytes and Neu7 astrocytes in vitro.

Graph shows average Intensity of SBA, MAA, SNA-I and WFA in primary astrocytes and Neu7 astrocytes (A). Mean \pm SEM. * = $P < 0.05$. Photomicrographs show SBA (B, C), MAA (D, E), SNA-I (F, G) and WFA (H, I) lectin staining in primary astrocytes and Neu7 astrocytes respectively. Scale bar = 30 μm .

Figure 3

Integrated density of SBA lectin staining in spinal cord slices.

Graph shows integrated density of SBA lectin staining in the white matter, gray matter and lesion site of uninjured, injured and injured spinal cords treated with CsA (A). Mean \pm SEM. * = $P < 0.05$.

Photomicrographs show SBA histochemical staining in the white matter (B, D, G), gray matter (C, E, H) and lesion site (F, I) of uninjured, injured and injured spinal cords treated with CsA respectively. Scale bar = 50 μm .

Figure 4

Integrated density of MAA lectin in spinal cord slices.

Graph shows integrated density of MAA lectin staining in the white matter, gray matter and lesion site sampling regions within uninjured, injured and injured spinal cords treated with CsA (A). Mean \pm SEM. * = $P < 0.05$.

Photomicrographs show MAA histochemical staining in the white matter (B, D, G), gray

matter (C, E, H) and lesion site (F, I) of uninjured, injured and injured spinal cords treated with CsA respectively. Scale bar = 50 μ m.

Figure 5

Integrated density of SNA-I lectin in spinal cord slices. Graph shows integrated density of SNA-I lectin staining in the white matter, gray matter and lesion site sampling regions within uninjured, injured and injured spinal cords treated with CsA (A). Mean \pm SEM.

Photomicrographs show SNA-I histochemical staining in the white matter (B, D, G), gray matter (C, E, H) and lesion site (F, I) of uninjured, injured and injured spinal cords treated with CsA respectively. Scale bar = 50 μ m.

Figure 6

Dual staining of astrocytes and SNA-I in injured spinal cord slices. Photomicrographs shows GFAP (red), SNA-I (green) and DAPI (blue) staining in the lesion site of spinal cord slices of injured and CsA- treated animals (A, C). Scale bar = 50 μ m. The boxed areas in A and C are magnified in B and D respectively. Scale bar = 20 μ m.

Figure 7

Dual staining of β I-integrin and SNA-I in injured spinal cord slices. Photomicrographs shows β I-integrin (red) and SNA-I (green) staining in the lesion site of spinal cord slices of injured and CsA-treated animals (A, C). Scale bar = 50 μ m. The boxed areas in A and C are magnified in B and D respectively. Scale bar = 20 μ m.

Figure 8

Integrated density of WFA lectin in spinal cord slices. Graph shows integrated density of WFA lectin staining in the white matter, gray matter and lesion site sampling regions within uninjured, injured and injured spinal cords treated with CsA (A). Mean \pm SEM. * = P < 0.05. Photomicrographs show WFA histochemical staining in the white matter (B, D, G), gray matter (C, E, H) and lesion site (F, I) of uninjured, injured and injured spinal cords treated with CsA respectively. Scale bar = 50 μ m.

Figure 9

Dual staining of GAP-43 and WFA in injured spinal cord slices. Photomicrographs shows GAP-43 (red), WFA (green) and DAPI (blue) staining in the lesion site of spinal cords of

injured and CsA-treated animals (A, C). Scale bar = 50 μm . The boxed area in A and C are magnified in B and D respectively. Scale bar = 20 μm .

Figure 10

Dual staining of Neurogranin and WFA in injured spinal cord slices. Photomicrographs shows Neurogranin (red) and WFA (green) staining in the lesion site of spinal cords in the injured and CsA-treated animals (A, D). Scale bar = 50 μm . A shows overview of white and gray matter. B and C show white and gray matter in injured spinal cord slice respectively. The boxed area from CsA-treated animal in D is magnified in E. Scale bar B, C and E = 20 μm .

Table 1. Lectins, their origin, their corresponding carbohydrate binding specificity and haptenic sugars. For histochemical inhibition experiments, lectins were co-incubated with 100 mM of the haptenic sugar and for lectin microarray printing, lectins were co-incubated in 1 mM of the haptenic sugar.

Abbreviation	Lectin	Origin	Binding specificity	Haptenic sugar
MAL-I	<i>Maackia amurensis</i> leucoagglutinin (MAL)	<i>Maackia amurensis</i>	Neu- α -(2 \rightarrow 3)-Gal- β -(1 \rightarrow 4)-GlcNAc-R, SO ₄ ²⁻ -3-Gal- β -(1 \rightarrow 4)-GlcNAc-R	Lac
MAL-II	<i>Maackia amurensis</i> hemagglutinin (MAH)	<i>Maackia amurensis</i>	Neu- α -(2 \rightarrow 3)-Gal- β -(1 \rightarrow 3)- (\pm Neu- α -(2 \rightarrow 6)-GalNAc, SO ₄ ²⁻ -3-Gal- β -(1 \rightarrow 3)-(\pm Neu- α -(2 \rightarrow 6)-GalNAc, SO ₄ ²⁻ -3-Gal- β -(1 \rightarrow R	Lac
SBA	Soybean agglutinin	<i>Glycine max</i>	Terminal α - or β -linked GalNAc, Gal	Gal
MAA	<i>Maackia amurensis</i> agglutinin	<i>Maackia amurensis</i>	Neu- α -(2 \rightarrow 3)-Gal- β -(1 \rightarrow 4)-GlcNAc-R, SO ₄ ²⁻ -3-Gal- β -(1 \rightarrow 4)-GlcNAc-R	Lac
SNA-I	<i>Sambucus nigra</i> isolectin-I	<i>Sambucus nigra</i> (elderberry)	Neu- α -(2 \rightarrow 6)-Gal(NAc)-R	Lac
WFA	<i>Wisteria floribunda</i> agglutinin	<i>Wisteria floribunda</i> (Japanese wisteria)	Terminal α - or β -linked GalNAc, lactose, Gal, chondroitin sulfate	Gal

Figure 1

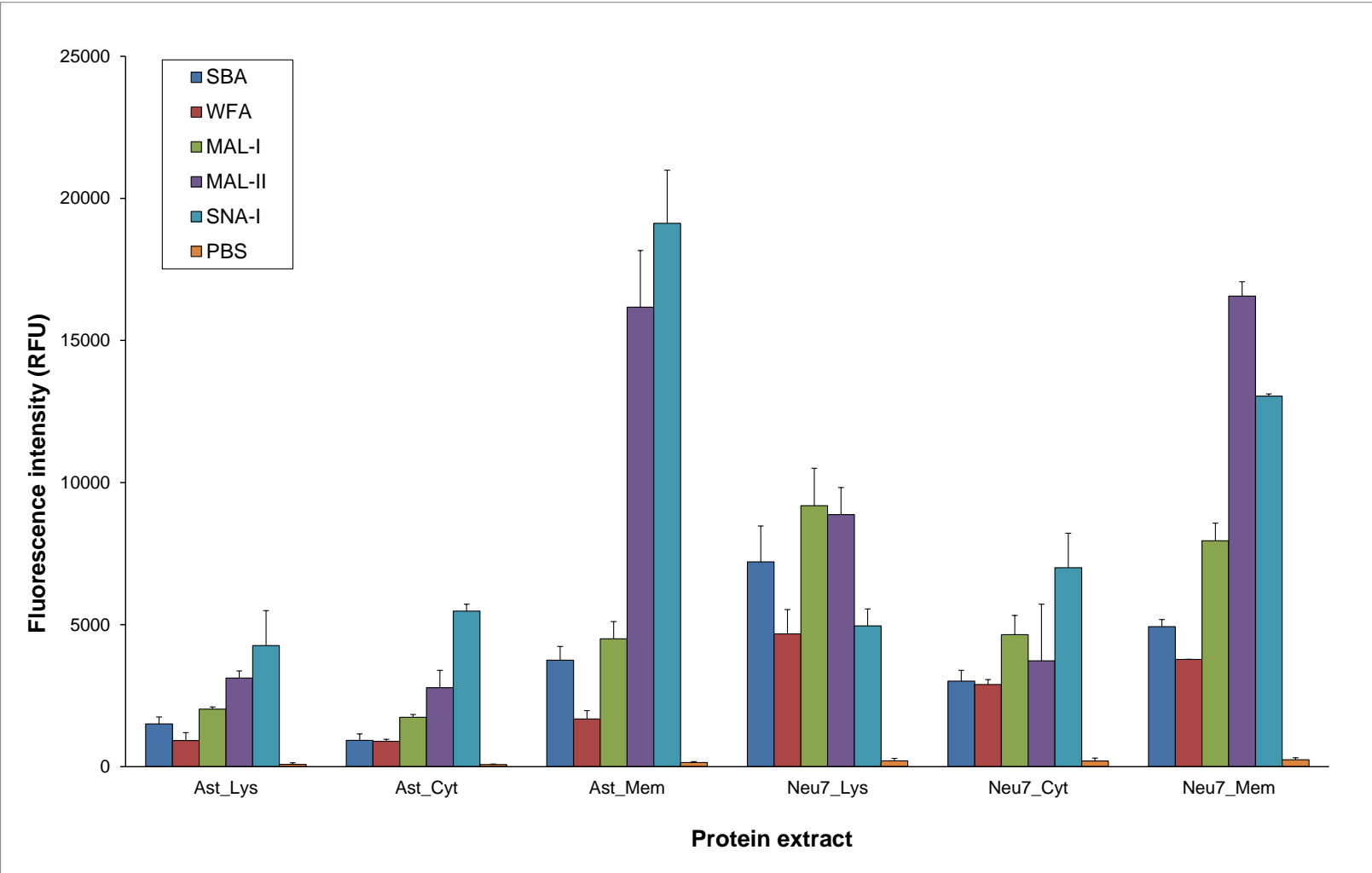


Figure 2

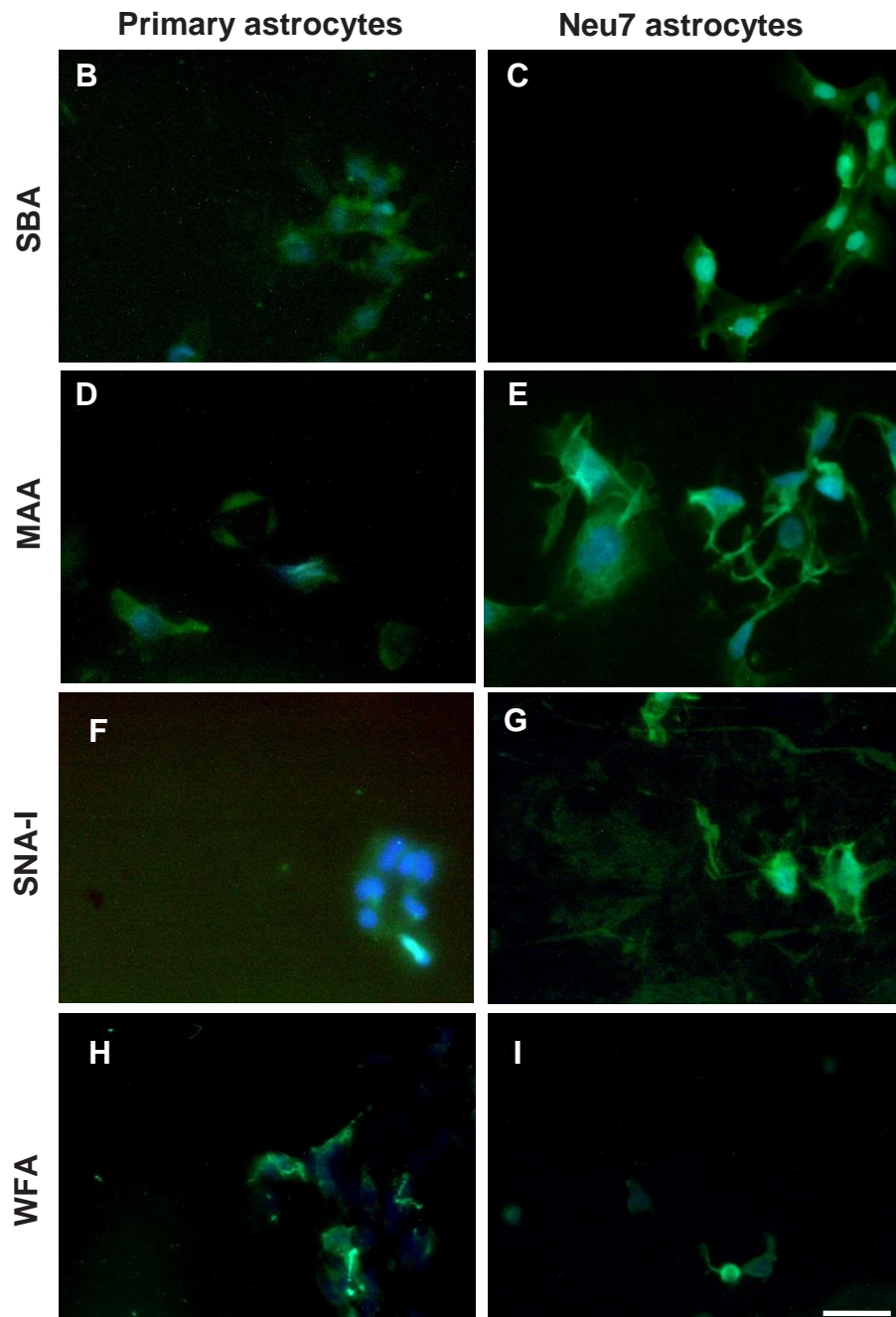
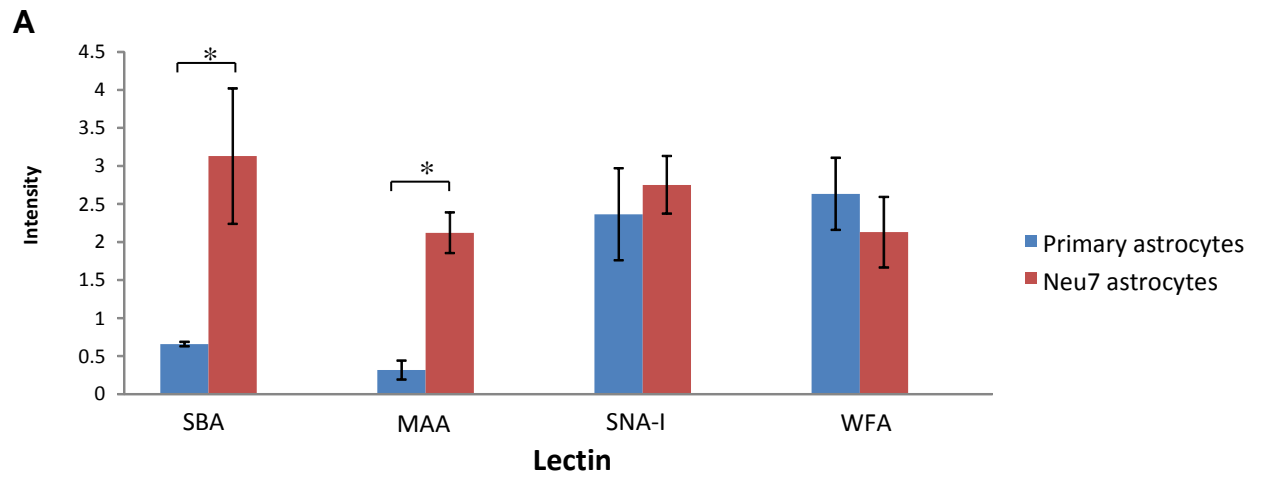


Figure 3

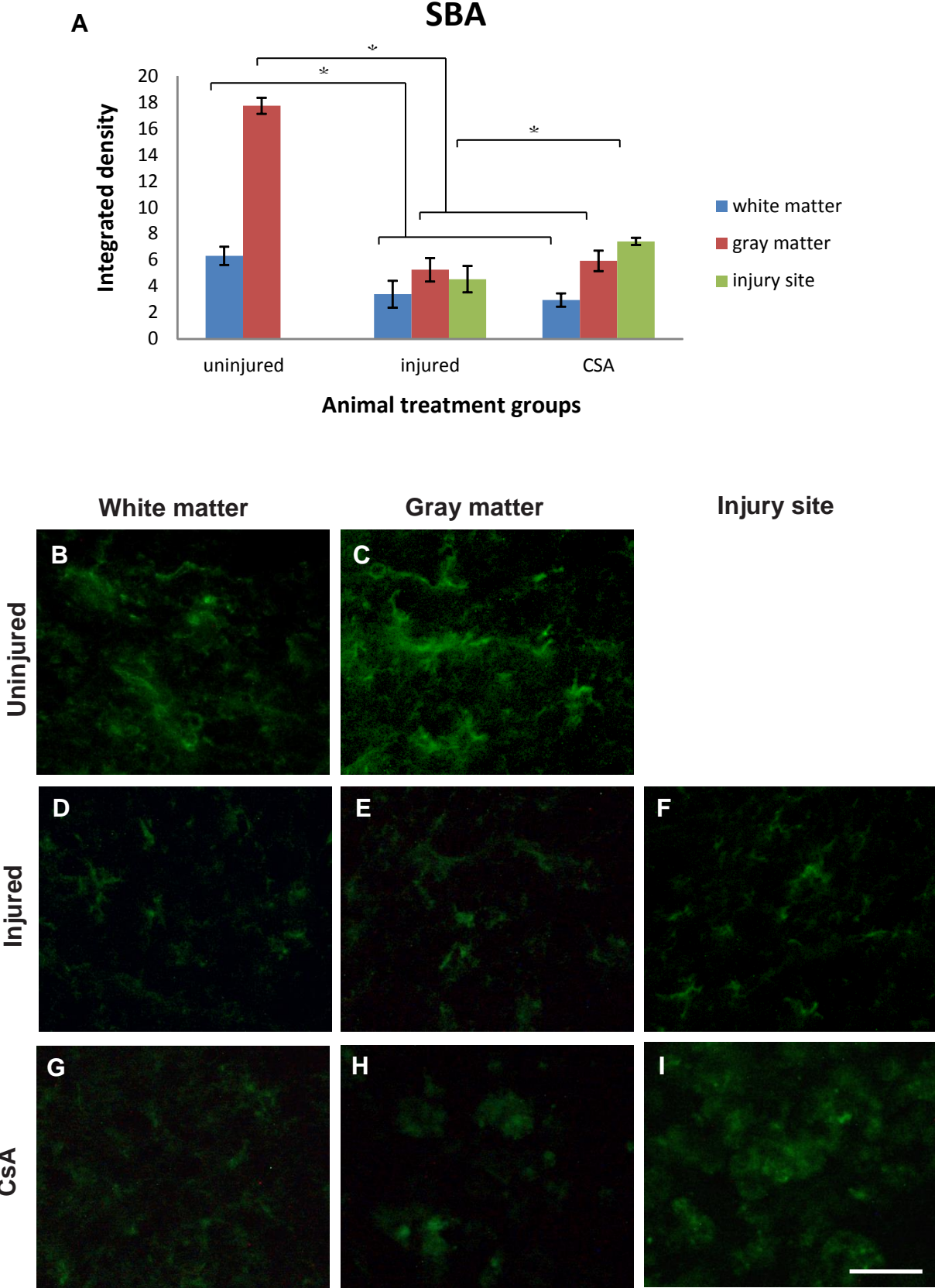


Figure 4

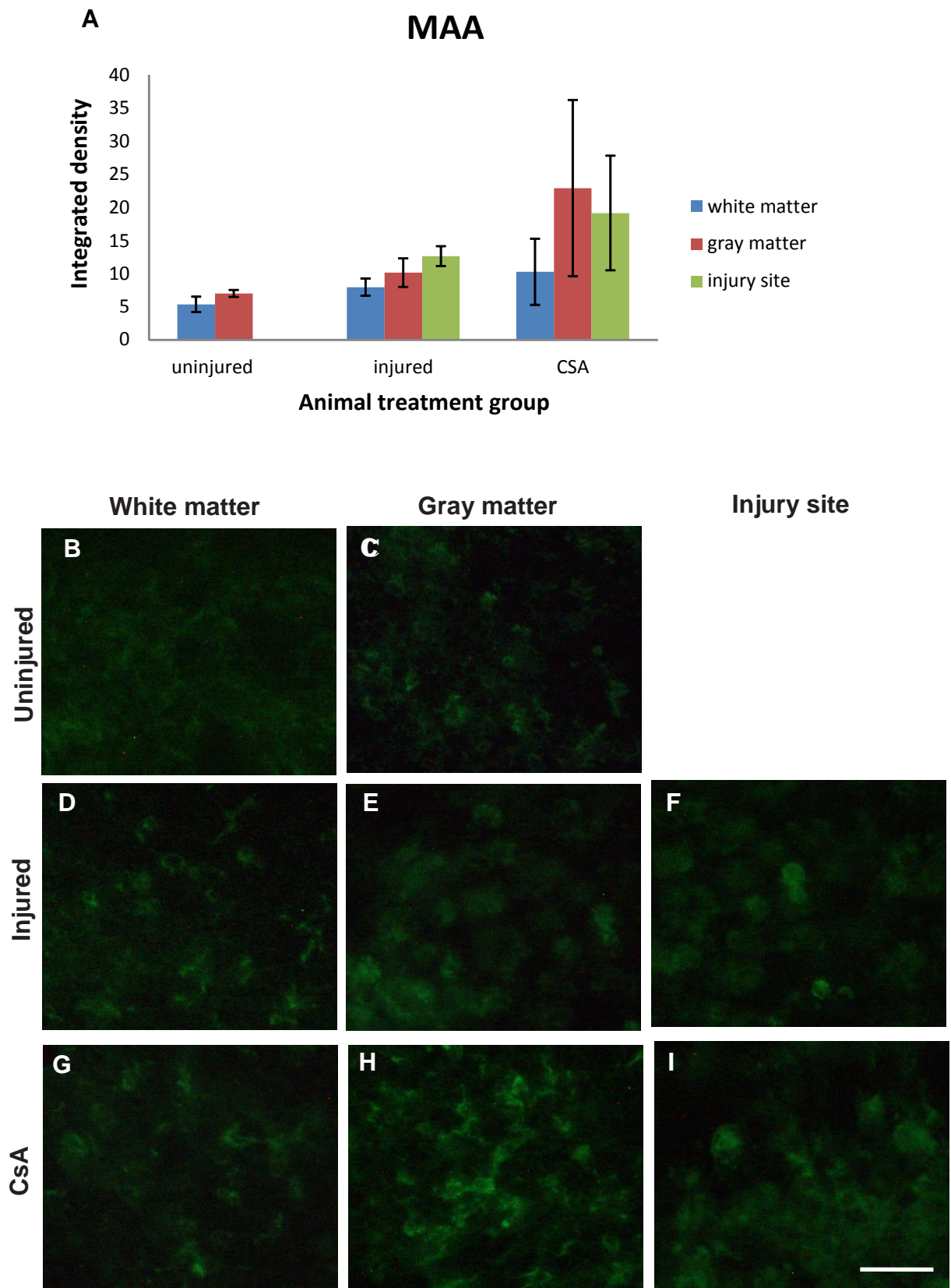


Figure 5

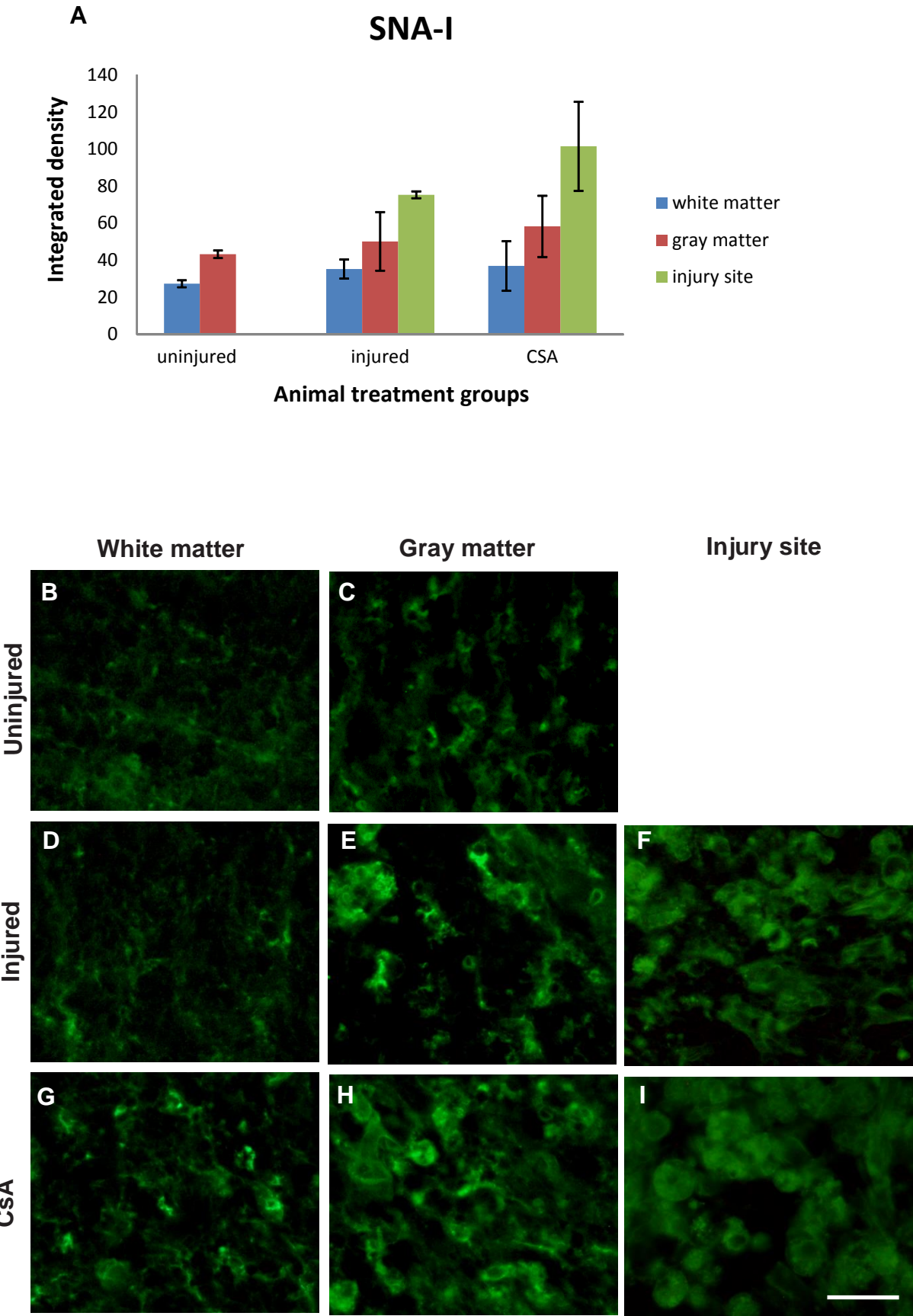


Figure 6. SNA-I lectin staining and GFAP immunohistochemical staining

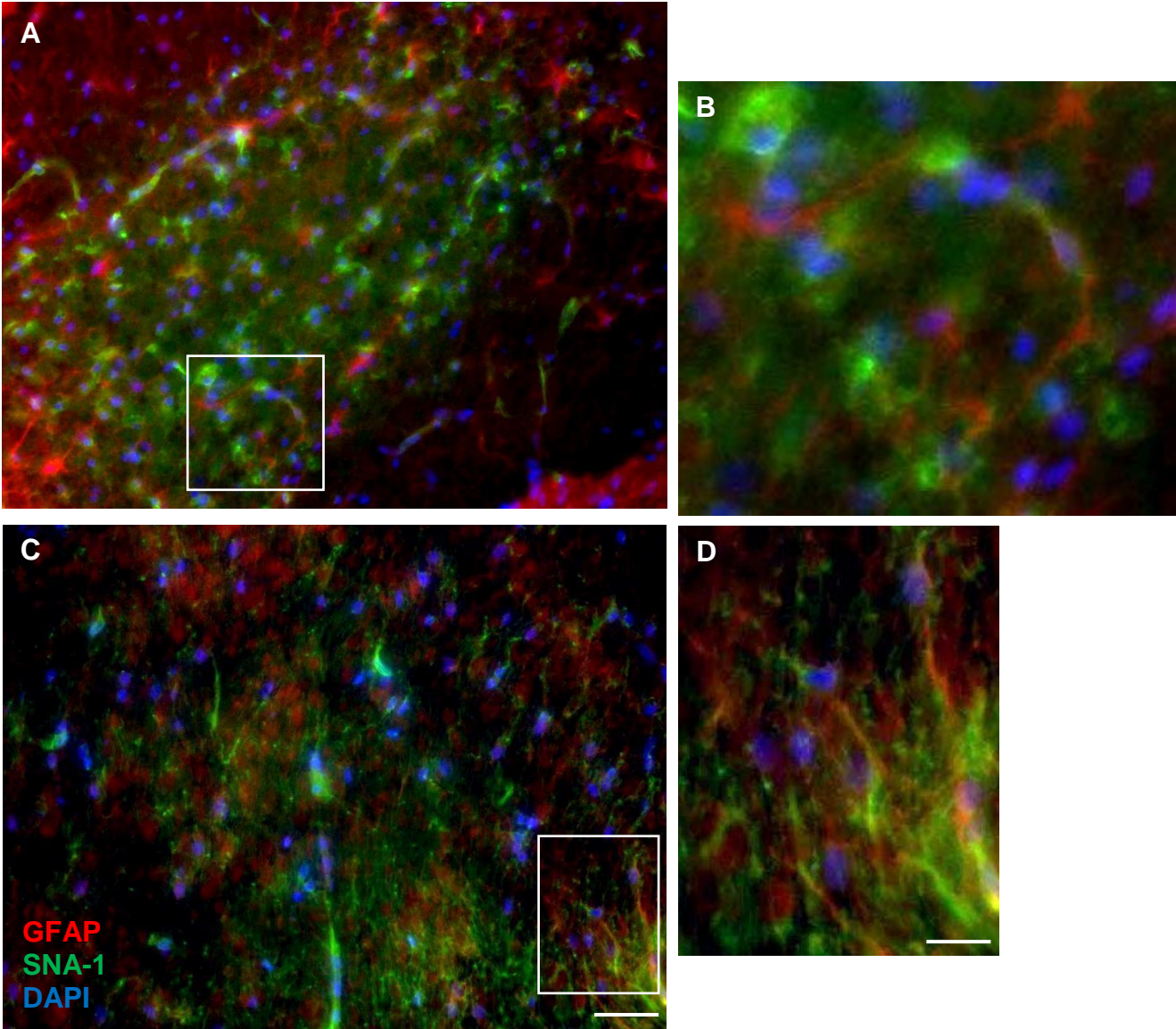


Figure 7. SNA-I lectin staining and β I integrin immunohistochemical staining

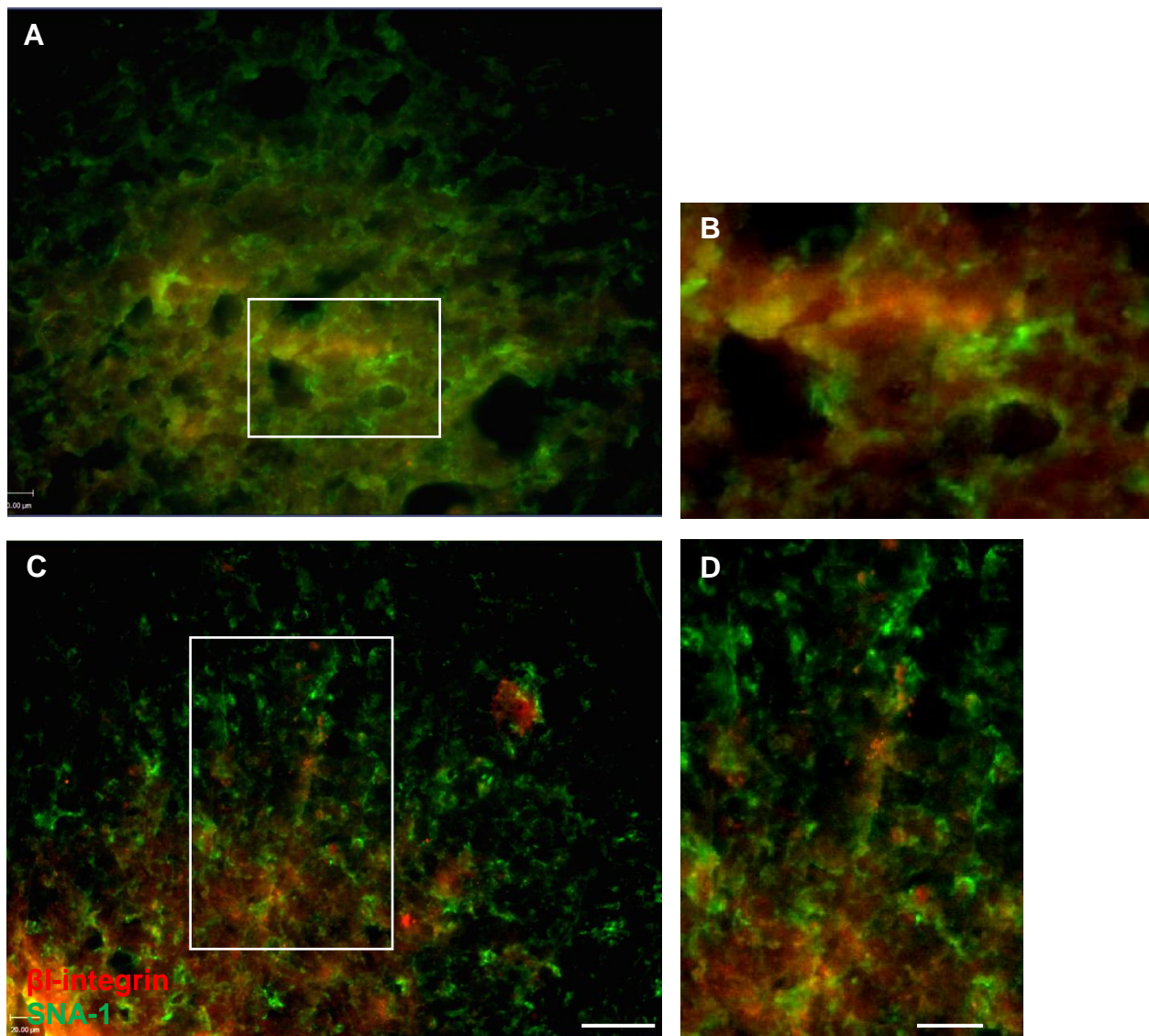


Figure 8

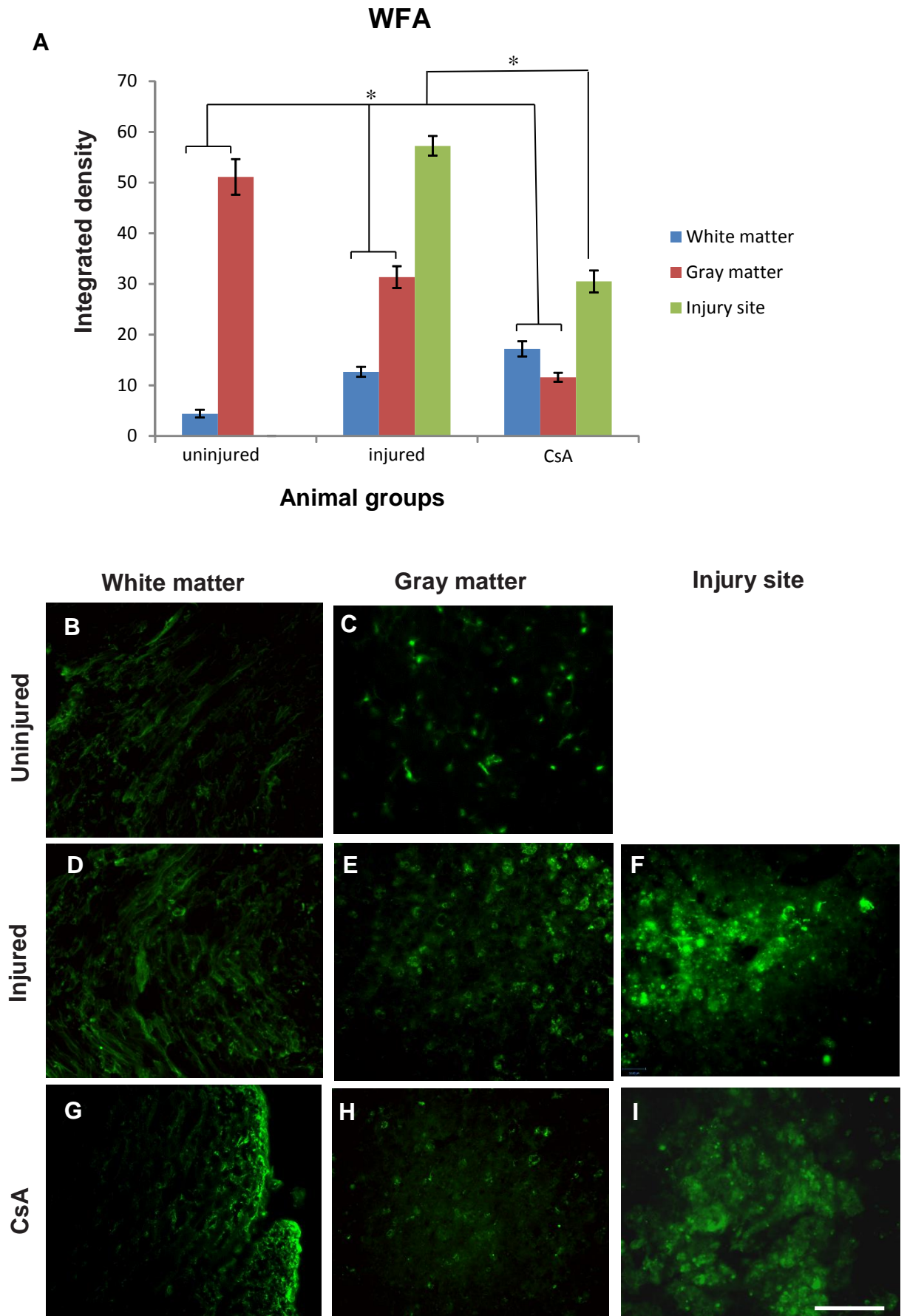


Figure 9. WFA lectin staining and GAP-43 immunohistochemical staining

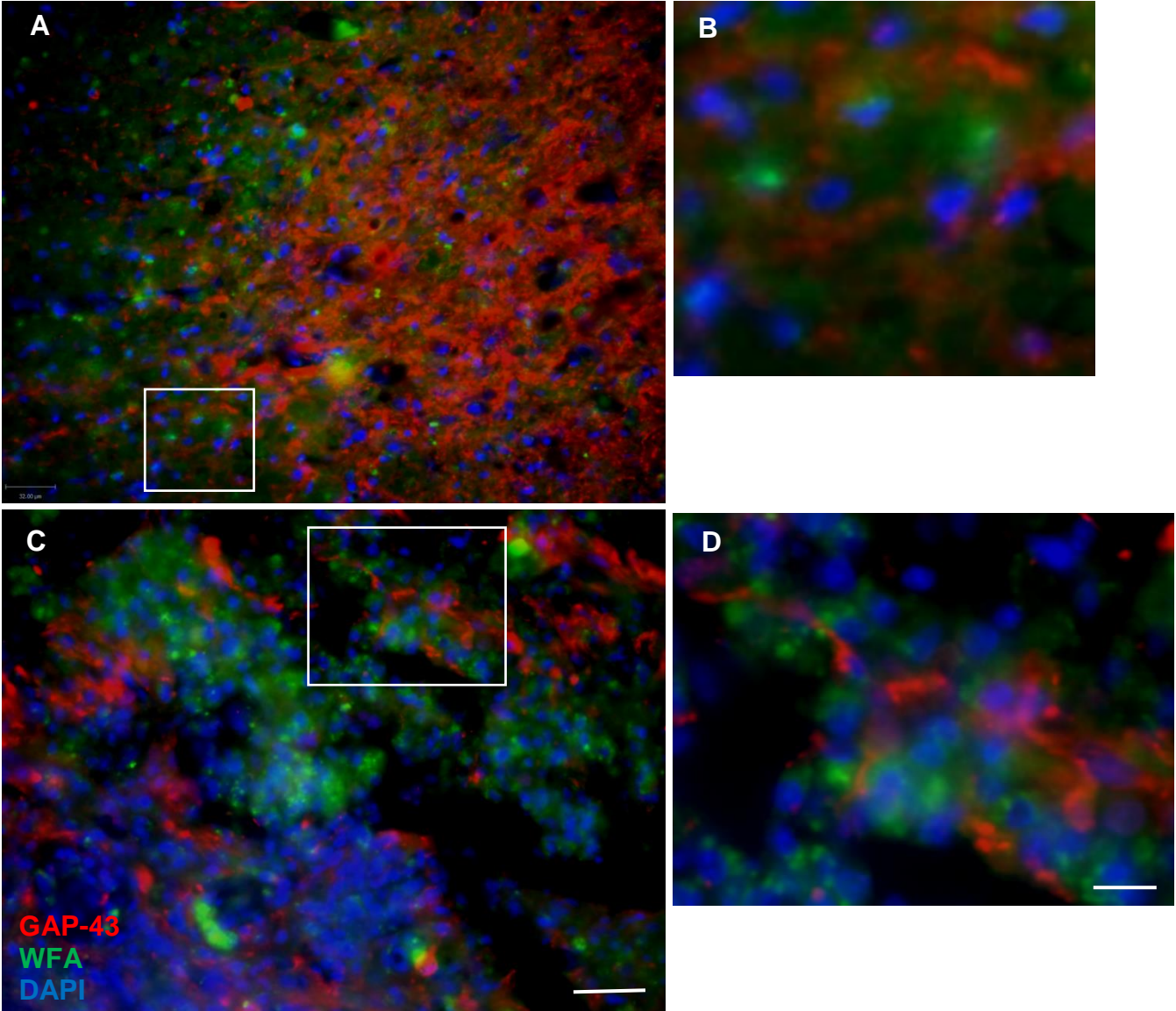
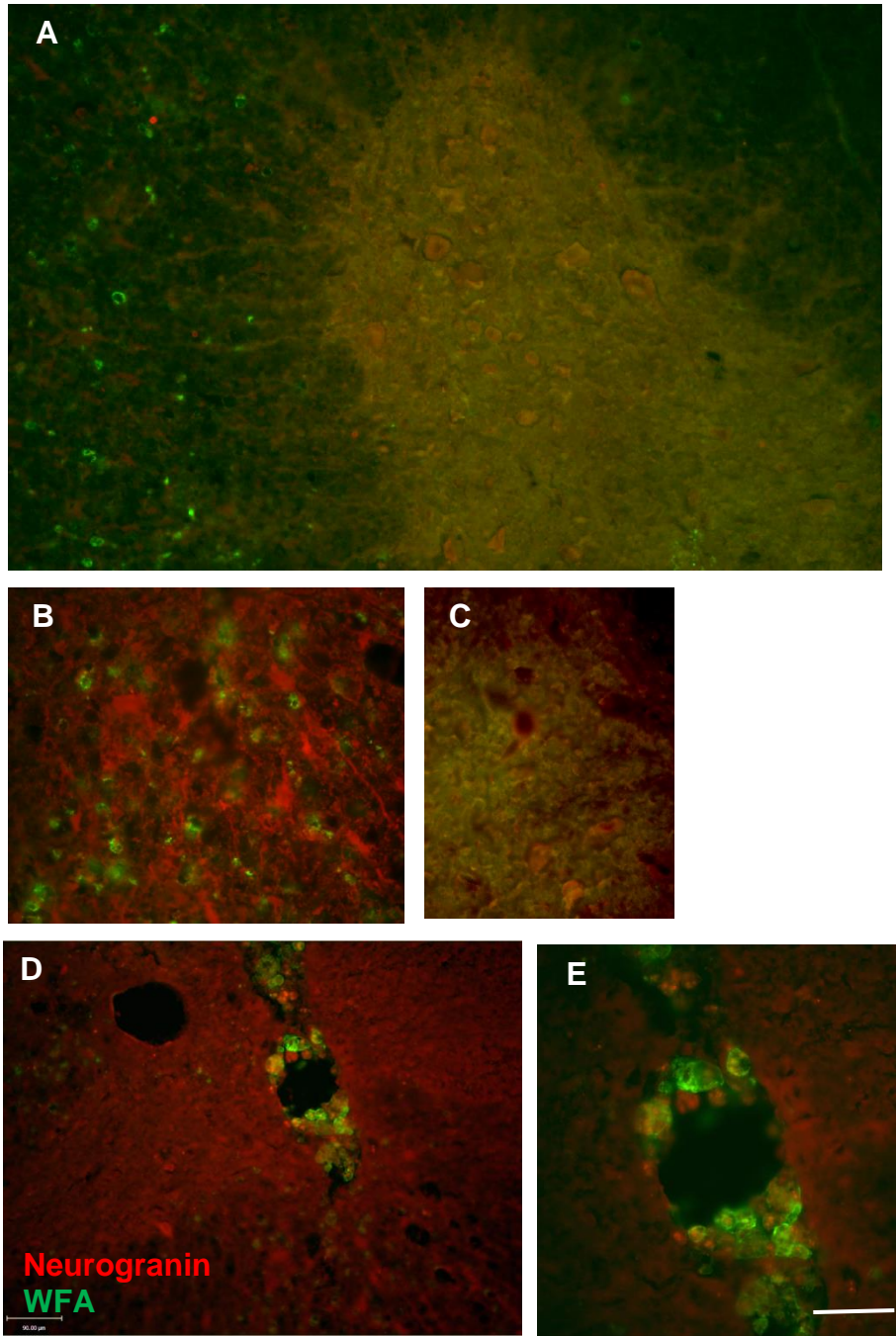


Figure 10. WFA lectin staining and neurogranin immunohistochemically staining



Graphical table of contents image

